Reptation Dynamics of Asymmetric Diblock Copolymer Melts via the Dynamic Random Phase Approximation

S. G. J. Mochrie

Departments of Physics and Applied Physics, Yale University, New Haven, Connecticut 06520

Received April 9, 2002

ABSTRACT: A calculation of the intermediate scattering function of an entangled melt of asymmetric diblock copolymers is presented. On the basis of the reptation model of polymer dynamics and the dynamic random phase approximation, it is shown that the spectrum of relaxation rates for an asymmetric diblock copolymer consists of two sets of modes. In the noninteracting case, both sets of modes have relaxation rates that are independent of the diblock composition. The relative mode amplitudes, however, depend strongly on composition. In the noninteracting case, one set has relaxation rates given by $\Gamma_{p,\beta} = \beta_p^2/t^*$, with $4t^*$ the disengagement time and β_p given by the pth positive root of $\beta_p \cot \beta_p - (qR_g)^2/2 = 0$, $p = 1$, 2, 3, ... The other set only appears in the asymmetric case, and, in both the small-qR_g and large-qR_g limits, has relaxation rates given by $\Gamma_{p,\alpha} = (\pi^2/4t^*)(2p - 2)^2$, $p = 2$, 3, 4, ...

Introduction

Block copolymers—composed of two or more distinct polymer constituents chemically bound together—bring together the properties of amphiphilic molecules and polymers. They exhibit a rich phase behavior,[1] which continues to excite interest as more components are incorporated,[2] as colloidal particles are added to create nanocomposites,[3] and as the material is confined in thin films,[4] etc. Beyond their time-averaged behavior, the dynamics of copolymer systems[5] reflect the motions of individual polymers, and it was recognized long ago that the study of block copolymer systems should permit detailed insights into fundamental aspects of not only the structure but also the dynamics of polymers via scattering measurements, because of the possibility that the different blocks may have different scattering strengths. A recent example is provided by photon correlation spectroscopy (PCS) measurements of the intermediate scattering function (IFS) for compositional fluctuations in the disordered phase of an entangled solution of a symmetric diblock copolymer.[6] The corresponding theoretical expression for the ISF was given in ref 6 and previously in ref 7, based on the dynamic random phase approximation and the reptation model of model dynamics, which it is believed should provide an appropriate description on length scales greater than the entanglement length.[8−10] In addition to polymer solutions, advances in the emerging technique of X-ray photon correlation spectroscopy (XPCS) suggest that it may soon be feasible to characterize the dynamics of block copoymer melts on length scales comparable to and smaller than the constituent polymers' radius of gyration (R_g).[11]

The goal of the current paper is to extend the calculation of the ISF given in ref 6 to include asymmetric diblock copolymers for comparison to future PCS, XPCS, or even neutron spin-echo (NSE) experiments. In the asymmetric case, it turns out, first, that a new family of dynamic modes emerges, which is not present in the symmetric case[12] and, second, that the ISF becomes increasingly non-single-exponential at the peak of the static structure factor for increasingly asymmetric compositions. Our results suggest that careful scattering studies, performed on asymmetric block copolymers, may afford an excellent opportunity to evaluate quantitatively the reptation model's detailed predictions for the higher-order mode relaxation rates and relative mode amplitudes. This is not only because of the predicted non-single-exponential relaxation of the ISF for very asymmetric block copolymers but also because of the point that when investigating entanglement effects, which become increasingly inportant as N increases, it is experimentally convenient that a diblock with a given Flory−Huggins interaction parameter (χ) remains in the homogeneous phase up to larger values of N for f far from $^1/_2$ than for f near $^1/_2$. For example, the instability toward phase separation occurs at $\chi N \simeq 10$ for $f \simeq {}^1/_2$, but at $\chi N \simeq 250$ for $f \simeq 0.05$.

Within the repation model, each polymer in a concentrated polymer system is supposed to be confined within a tube delineated by the path of the polymer in question and created by entanglements with neighboring polymers. (The polymer molecular weight must be sufficiently large in order for entanglements to be important. In a melt, for example, the component polymers must exceed the entanglement molecular weight, which typically corresponds to an entanglement polymerization index of $N_e \simeq 100-200$.) Reptation is diffusion along the tube created by entanglements. If the polymer is assumed to have a fixed contour length, the characeristic time for disengagement from the tube that exists at time zero is estimated as $\tau_d \simeq L^2/D_C$, where L is the contour length and D_C is the diffusion coefficient along the tube. Actually, there are fluctuations in the polymer's contour length, which permit a more rapid escape. Specifically, Doi and Edwards have shown that when contour length fluctuations are included, the disengagment time becomes renormalized to $\tau_d \simeq (1 - X/\sqrt{N_e/N})^2 L^2/D_C$, where X is a numerical constant greater than 1.47, N is the polymerization index,[10] and N_e is the entanglement polymerization index. The origin of this renormalization is that as the contour length fluctuates, the chain ends retract and extend, thus creating new tube ends in a fashion that does not depend on reptation. This effectively renormalizes the length of chain involved in reptation and hence the disengagement time.

10.1021/ma020565a CCC: $25.00
Published on Web 06/03/2003

For highly asymmetric diblocks, however, for which one of the blocks is more-or-less at the chain end, and therefore escapes the initial tube via contour length fluctuations instead of by reptation, one might reasonably ask what role does reptation have in relaxing compositional fluctuations or in determining the IFS? Specifically, one might argue that since the scattering contrast comes from labeled chain ends that do not reptate, the IFS of such a system should not reflect the reptational dynamics of the unlabeled chain centers. This reasoning is incorrect, however, as may seen by an appeal to Babinet's principle, which states that the scattering from the complement of an object is the same as the scattering from the object itself, so that it is equally permissible to envision the scattering contrast to originate in the longer blocks, which surely reptate. To understand why reptation and the calculation of the present paper is indeed relevant, even for highly asymmetric diblocks, it is important to realize that the decay of $S(Q, t)$ to zero only occurs when the final compositional inhomogenieity at time t becomes uncorrelated with the initial compositional inhomogeneity at time 0. Since the central portion of diblock is composed of (e.g.) A monomers, the initial locations of the polymers' centers will remain A-rich until the central portion of each polymer has moved, which will occur via reptation (for sufficiently high molecular weight polymers). That is, to completely relax compositional fluctuations, the initial tube must disappear, not just part of it, irrespective of the polymer composition. By this line of reasoning, the final disappearance of correlations at long times, even in a very asymmetric diblock takes place as prescribed by the reptation model and worked out in this paper.

In addition to tube escape, so-called Rouse modes within the tube give rise to the rapid partial relaxation of short distance compositional fluctations. Nevertheless, on the long time scales relevant to reptation, it is simply as though the polymer composition is averaged over the cross section of the tube.[13] It follows that on these time scales, the effect of the Rouse modes is to modify the ISF by an additional factor, $P_R(q)$, characterized by the tube diameter, d. Specifically, ref 13 suggests

$$P_R(q) = e^{-q^2d^2/36} \tag{1}$$

At small qd, P_R deviates only slightly from unity. For polymer melts, d is typically 50 Å. Thus, for sufficiently high molecular weight diblocks, there exists a region of q for which $qR_g \gg 1$ and yet $qd \ll 1$, so that the important compositional fluctuations around the peak of the structure factor relax mainly via reptation. Relaxation within the tube and the resultant $P_R(q)$ has been characterized experimentally for polymer melts, for example, via beautiful NSE experiments.[14−17] Reference 17, in particular, explores in detail the region of phase space where the ISF shows significant decays as a result of Rouse modes and contour length fluctuations. In the following, it should be understood that our results apply at times that are much longer than those characteristic of Rouse modes and that, for simplicity, we have omitted $P_R(q)$ from the formulas presented. In addition, it should be understood that our results apply only for highly entangled polymers with polymerization index sufficiently greater than N_e, so that contour fluctuations contribute little to the decay of the IFS, as found experimentally in ref 17. In principle, the scheme for accounting for contour length fluctuations introduced in ref 17 could be applied to the final results obtained here. However, this is outside of the scope of the present paper. Another, slightly different effect, peculiar to block copolymers, which should be considered in a complete theory, is that, on the reptation time scale, Rouse motions along the tube will smear out the sharp junction between A monomers and B monomers.

We also neglect polydispersity, assuming that our copolymer melt is perfectly monodisperse. Fortunately, there exists a recent comprehensive review of diblock copolymer dynamics[5] to which the reader is referred for a more complete discussion of such topics as the partial relaxation of compositional fluctuations via Rouse modes, or the so-called polydispersity mode.

Theoretical Approach

According to the dynamic random phase approximation (dRPA), the collective response of a melt of copolymers composed of A and B monomers, accounting only for excluded volume interactions, is related to the single chain response via

$$\kappa_0(q,s) = \frac{\kappa_{AA}(q,s)\kappa_{BB}(q,s) - \kappa_{AB}^2(q,s)}{\kappa_{AA}(q,s) + \kappa_{BB}(q,s) + 2\kappa_{AB}(q,s)} \tag{2}$$

where q is the wavevector, s is the Laplace frequency, κ_{AA} is the single chain response function, describing how the density of A monomers changes in response to an applied field coupling to A monomers, κ_{BB} is the analogous quantity except for B monomers, and κ_{AB} is the single chain response functions describing how the density of A monomers changes in response to an applied field coupling to B monomers.[18]

The fluctuation−dissipation theorem, in turn, informs us that each of these response functions is related to the corresponding IFS [$S(q,t)$]. Specifically, in the case that the Laplace frequency-dependent susceptibility exhibits simple poles, the ISF is given by

$$S(q,t) = S(q)\sum_{p=1}^{\infty} C_p \exp(-\Gamma_p t) \tag{3}$$

where $S(q) = S(q,0)$ is the static structure factor, and the mode decay rates [$\Gamma_p = \Gamma_p(q)$] correspond to the poles of κ, that is

$$\kappa^{-1}(q, s = -\Gamma_p) = 0 \tag{4}$$

while the relative mode amplitudes [$C_p = C_p(q)$] are related to the corresponding residues

$$C_p = \frac{1}{S(q)\Gamma_p}(\text{residue})\kappa(q, s = -\Gamma_p) \tag{5}$$

For comparison to PCS or NSE measurements, it is most useful to present results for the ISF, that is, to characterize the sample dynamics in the time domain. This is because the ISF is directly measured in NSE experiments, while the square of the ISF is measured in PCS experiments. Under some circumstances, however, it may instead be useful to express the sample dynamics in the frequency domain, via the dynamic structure factor, $S(q,\omega)$, which is simply the frequency Fourier transform of the ISF.[19] It follows that the dynamic structure factor corresponding to the ISF of eq

3 is

$$S(q,\omega) = \sum_{p=1}^{\infty} \frac{2C_p\Gamma_p}{\omega^2 + \Gamma_p^2} \tag{6}$$

The third ingredient in our calculation is the monomer−monomer dynamic correlation function for monomers n and m on a N-monomer chain, which according to the reptation model, is given by

$$S_{nm}(q,t) = \sum_{p=1}^{\infty} \frac{2\mu}{A_p} \cos[2\alpha_p(n/N - {}^1/_2)] \times \cos[2\alpha_p(m/N - {}^1/_2)] \exp(-\alpha_p^2 t/t^*) + \frac{2\mu}{B_p} \times \sin[2\beta_p(n/N - {}^1/_2)] \sin[2\beta_p(m/N - {}^1/_2)] \exp(-\beta_p^2 t/t^*) \tag{7}$$

where $\mu = (qR_g)^2/2$ with R_g being the polymer's radius of gyration, α_p is the pth root of

$$\alpha_p \tan \alpha_p - \mu = 0 \tag{8}$$

β_p is the pth root of

$$\beta_p \cot \beta_p + \mu = 0 \tag{9}$$

$A_p = \mu^2 + \mu + \alpha_p$, $B_p = \mu^2 + \mu + \beta_p$, and $t^* = \tau_d/4$ with τ_d the disengagement time.[10] The corresponding monomer−monomer response function is obtained via Laplace transformation of the result that $\kappa(q,t) = -\theta(t)\partial S(q,t)/\partial t$, where $\theta(t)$ is zero for $t > 0$ and unity otherwise:

$$\kappa_{nm}(q,s) = \sum_{p=1}^{\infty} \frac{2\mu}{t^*A_p(s + \alpha_p^2/t^*)} \cos[2\alpha_p(n/N - {}^1/_2)] \times \cos[2\alpha_p(m/N - {}^1/_2)] + \frac{2\mu}{B_p(s + \beta_p^2/t^*)} \times \sin[2\beta_p(n/N - {}^1/_2)] \sin[2\beta_p(m/N - {}^1/_2)] \tag{10}$$

Results

In general, to obtain κ_{AA}, for example, from eq 10, we must sum n and m in eq 10 over all values corresponding to A monomers, depending on the polymers' architecture. Specializing to a diblock copolymer for which $1 \le n < fN$ are A monomers and the remaining are B monomers and transforming the sum to an integral gives the result that

$$\kappa_{AA}(q,s) = \sum_{p=1}^{\infty} \left[\frac{2\mu I_{1p}^2}{t^*A_p(s + \alpha_p^2/t^*)} + \frac{2\mu I_{2p}^2}{t^*B_p(s + \beta_p^2/t^*)} \right] \tag{11}$$

where $I_{1p} = \sin \alpha_p + \sin[(2f - 1)\alpha_p]$ and $I_{2p} = \cos \beta_p - \cos[(2f - 1)\beta_p]$. κ_{BB} and κ_{AB} are obtained similarly as

$$\kappa_{BB}(q,s) = \sum_{p=1}^{\infty} \left[\frac{2\mu I_{3p}^2}{t^*A_p(s + \alpha_p^2/t^*)} + \frac{2\mu I_{4p}^2}{t^*B_p(s + \beta_p^2/t^*)} \right] \tag{12}$$

and

$$\kappa_{AB}(q,s) = \sum_{p=1}^{\infty} \left[\frac{2\mu I_{1p} I_{3p}}{t^*A_p(s + \alpha_p^2/t^*)} + \frac{2\mu I_{2p} I_{4p}}{t^*B_p(s + \beta_p^2/t^*)} \right] \tag{13}$$

where $I_{3p} = \sin \alpha_p - \sin[(2f - 1)\alpha_p]$ and $I_{4p} = -I_{2p}$.

Equations 11−13 may be combined as prescribed by eq 2, yielding

$$\kappa_0 = \Sigma_\beta + \Sigma_\alpha \tag{14}$$

where

$$\Sigma_\beta = \sum_{p=1}^{\infty} I_{2p}^2/b_p \tag{15}$$

and

$$\Sigma_\alpha = \sum_{p=1}^{\infty}\sum_{r=1}^{\infty} \frac{I_{1p}I_{3r}(I_{1p}I_{3r} - I_{1r}I_{3p})/(a_p a_r)}{\sum_{u=1}^{\infty} (I_{1u} + I_{3u})^2/a_u} \tag{16}$$

with $a_p = t^*A_p(s + \alpha_p^2/t^*)/2\mu$ and $b_p = t^*B_p(s + \beta_p^2/t^*)/2\mu$. It is significant that terms in Σ_α with $p = r$ vanish.

Equations 14−16 constitute an explicit functional form for the dynamic susceptibility of a copolymer melt interacting via excluded volume interactions only. To the extent that the interaction parameter between hydrogenated and deuterated monomers may be neglected, this result applies to the important case of chemical homopolymers, that are actually composed of two blocks, one deuterated (D) and the other hydrogenated (H).[20] At present, the longest time scales accessible to NSE (10^{-7} s) are probably still too fast to study reptation in melts directly. However, it may be noted that these longest times have increased by a factor of nearly 100 over the past decade and there may be significant future improvements.

A check on our result for κ_0 follows from the fact that the zero frequency limit of the response function, $\kappa(q,0)$, is equal to the zero-time limit of the ISF, $S(q,0)$, which is the static structure factor, $S(q)$. Figure 1 shows three diblock copolymer structure factors so-obtained. The top panel shows $S(q)/N$ for a noninteracting, symmetric ($f = {}^1/_2$) diblock melt. The middle panel shows $S(q)/N$ for a noninteracting, asymmetric diblock melt with $f = 0.05$. The bottom panel shows $S(q)/N$ for an interacting, asymmetric diblock melt with $f = 0.05$ and an interaction parameter of $\chi = 0.23$ (see below), which is near the stability boundary. These plots reproduce Leibler's results for the static structure factor of a melt of diblock copolymers.[21]

Equations 14−16 imply that, for the H−D diblock melts described above, we may expect that the spectrum of collective-mode decay rates measured in a neutron scattering experiment, for example, to consists of two sets, with each set given by the poles of Σ_β and Σ_α, respectively. Clearly, the first set of relaxation rates—those corresponding to Σ_β—are given by $\Gamma_{p,\beta} = \beta_p^2/t^*$ for $p = 1, 2, 3, 4, \ldots$. It follows that this set of relaxation rates does not depend on f. Equation 9 reveals that, in the small-qR_g limit, $\beta_p \simeq (2p - 1)\pi/2$, and, in the large-$qR_g$ limit, $\beta_p \simeq p\pi$. Therefore, $\Gamma_{p,\beta} \simeq (2p - 1)^2\pi^2/(4t^*)$ at small qR_g, and $\Gamma_{p,\beta} \simeq (2p)^2\pi^2/(4t^*)$ at large qR_g for $p = 1, 2, 3, 4, \ldots$.

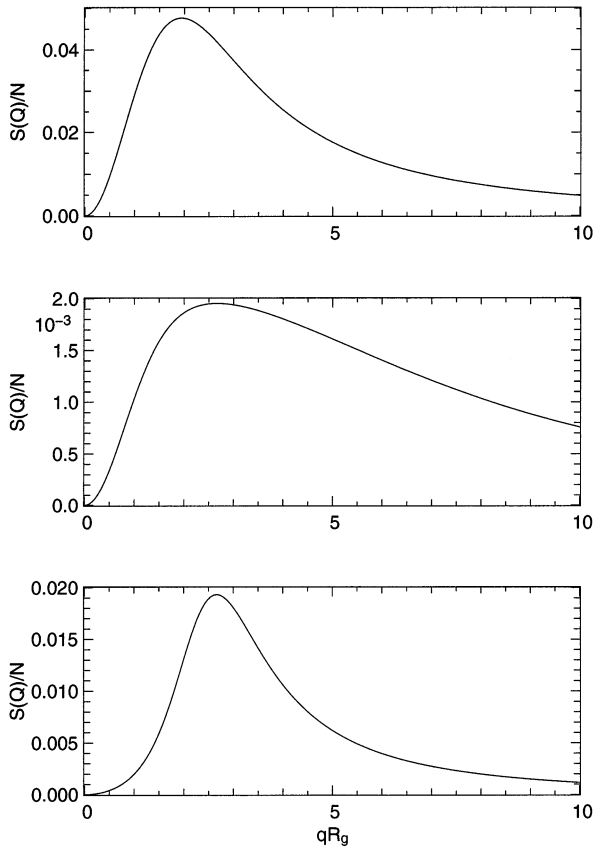

Figure 1. Top: $S(q)/N$ vs qR_g for a noninteracting diblock copolymer melt with $f = {}^1/_2$. Middle: $S(q)/N$ vs qR_g for a noninteracting diblock copolymer melt with $f = 0.05$. Bottom: $S(q)/N$ vs qR_g for an interacting diblock copolymer melt with $f = 0.05$ and $\chi N = 230$.

In contrast, a simple expression is not available in general for the decay rates corresponding to Σ_α. Nevertheless, it is instructive to write

$$\Sigma_\alpha = \frac{\Pi_v a_v \sum_{p=1}^{\infty}\sum_{r=1}^{\infty} I_{1p}I_{3r}(I_{1p}I_{3r} - I_{1r}I_{3p})/(a_p a_r)}{\Pi_v a_v \sum_{u=1}^{\infty}(I_{1u} + I_{3u})^2/a_u} = \frac{\sum_{p=1}^{\infty}\sum_{r=1}^{\infty} I_{1p}I_{3r}(I_{1p}I_{3r} - I_{1r}I_{3p})\Pi_{v\neq p,r} a_v}{\sum_{u=1}^{\infty} 4 \sin^2 \alpha_u \Pi_{v\neq u} a_v} \quad (17)$$

By the manner in which it is constructed, the numerator of eq 17 does not exhibit any poles. It follows that the poles of Σ_α correspond to the roots of the denominator of eq 17 (D_α):

$$D_\alpha = \sum_{u=1}^{\infty} 4 \sin^2 \alpha_u \Pi_{v\neq u} a_v \quad (18)$$

Since D_a is explicitly independent of f, its roots are independent of f, so that the corresponding $\Gamma_{p,\alpha}$ relaxation rates are also independent of f. Because terms in eq 17 with $p = r$ vanish, there does not appear a relaxation rate for $p = 1$. This is as it should be, because this mode would be diffusive at small qR_g. However, there are no long-length-scale compositional fluctuations in this system, so that there cannot be diffusive modes.

In the small-qR_g limit, the numerator of Σ_α is dominated by terms with either $p = 1$ or $r = 1$, while the denominator is dominated by the term with $u = 1$. In this case only, it follows that

$$\Sigma_\alpha \simeq 2I_{11}/(I_{11} + I_{31}) \sum_{p=2}^{\infty} I_{3p}(I_{11}I_{3p} - I_{1p}I_{31})/a_p \quad (19)$$

and the second set of relaxation rates is given by $\Gamma_{p,\alpha} = \alpha_p{}^2/t^*$ for $p = 2, 3, 4, ...$, corresponding to the zeros of a_p. In the small-qR_g limit, eq 8 shows that $\alpha_p \simeq (p - 1)\pi$, so that, at small qR_g, $\Gamma_{p,\alpha} \simeq (2p - 2)^2\pi^2/(4t^*)$, for $p = 2, 3, 4, ...$

To obtain an approximate expression for $\Gamma_{p,\alpha}$ in the large qR_g-limit, it is useful to invoke the result that $\alpha_p = \pi(2p - 1)/2$ at large qR_g,,[10] so that $\sin^2 \alpha_p = 1$. In addition, it turns out that, instead of examining D_α, it is convenient to examine

$$D'_\alpha = \sum_{p=1}^{\infty} 4 \sin^2 \alpha_p/a_p \quad (20)$$

which exhibits the same roots as D_α. Using eq 1.421.1 of ref 22, we find

$$D'_\alpha = \sum_{p=1}^{\infty} 4/(s - \alpha_p{}^2/t^*) = \sum_{p=1}^{\infty} \frac{t^*/\pi^2}{st^*/4\pi^2 - (2p - 1)^2} = -2t^*\sqrt{|s|t^*}\tan\sqrt{|s|t^*} \quad (21)$$

Thus, in the large-qR_g limit, the $\Gamma_{p,\alpha}$ are given by $\tan \sqrt{\Gamma_{p,\alpha}t^*} = 0$. We may deduce that $\Gamma_{\alpha,p} = (2p - 2)^2\pi^2/(4t^*)$ for $p = 2, 3, 4, ...$, which happens to also be the small qR_g-limit of $\Gamma_{\alpha,p}$.

To compare our results to those of ref 6, we specialize briefly to the case of a symmetric diblock with $f = {}^1/_2$. It then follows that $I_{1p} = I_{3p} = \sin \alpha_p$, so that Σ_α vanishes and the dynamic susceptibility reduces to

$$\kappa_0(q,s) = \sum_{p=1}^{\infty} I_{2p}{}^2/b_p = \sum_{p=1}^{\infty} (1 - \cos \beta_p)^2/b_p \quad (22)$$

It follows from eq 22 that

$$S_0(q,t) = \sum_{p=1}^{\infty} \frac{2\mu I_2{}^2}{\beta_p{}^2 B_p} \exp(-\beta_p{}^2 t/t^*) = \sum_{p=1}^{\infty} \frac{2\mu(1 - \cos\beta_p)^2}{\beta_p{}^2(\mu^2 + \mu + \beta_p)} \exp(-\beta_p{}^2 t/t^*) \quad (23)$$

which reproduces the result given in ref 6 for a symmetric diblock. Evidently, the second set of modes—the $\Gamma_{p,\alpha}$—are absent for symmetric diblocks. In this sense, the spectrum of a melt of asymmetric diblocks is fundamentally different from that of a melt of symmetric diblocks.

Figure 2 shows the calculated relaxation rates of the lowest four modes of a symmetric diblock copolymer ($f = {}^1/_2$) plotted in units of $\pi^2/(4t^*)$ vs qR_g. In the small-qR_g limit, the relaxation rates are given by $\Gamma_{p,\beta} \simeq (2p -$

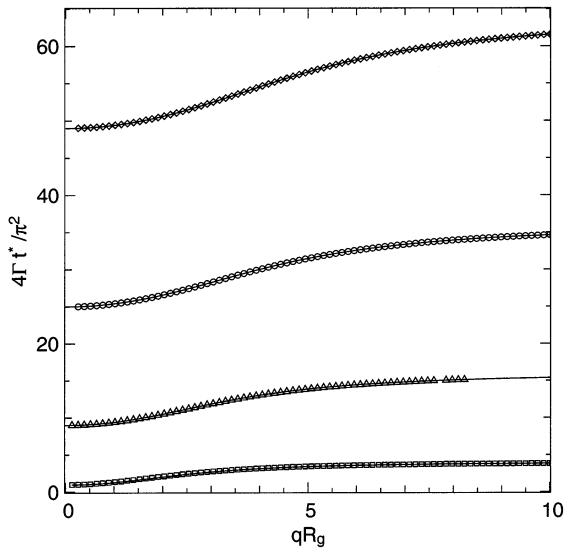

Figure 2. Calculated relaxation rates for the lowest four modes of a noninteracting, symmetric diblock copolymer ($f = {}^1/_2$) plotted in units of $\pi^2/(4t^*)$ vs qR_g.

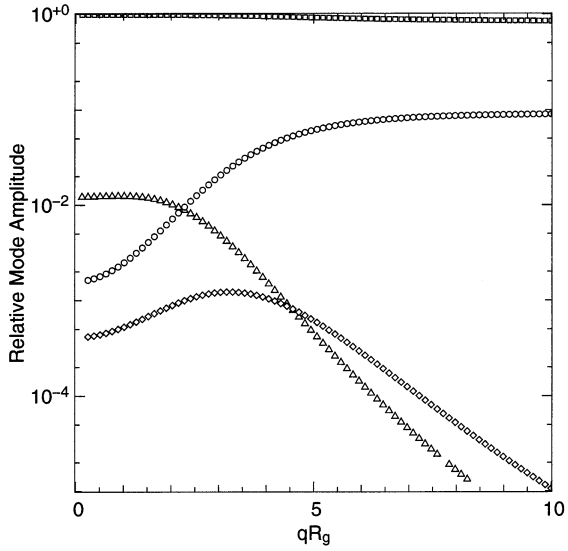

Figure 3. Calculated mode amplitudes for the lowest four modes of a noninteracting, symmetric diblock copolymer, corresponding to the relaxation rates shown in Figure 2.

$1)^2\pi^2/(4t^*)$, $p = 1, 2, 3, ...$, as noted in ref 6. With increasing qR_g, the rates increase monotonically to approach the large-qR_g limit of $\Gamma_{p,\beta} \simeq (2p)^2\pi^2/(4t^*)$, $p = 1, 2, 3, ...$ The corresponding relative mode amplitudes $[C_p(q)]$ are shown in Figure 3 plotted on a logarithmic scale vs qR_g plotted on a linear scale. The $\Gamma_{1,\beta}$-mode has a relative amplitude of nearly unity at all values of qR_g studied. Thus, in the symmetric case, the ISF deviates only slightly from a single-exponential decay. The amplitudes of the higher-order modes with $p = 2$ and 4 decrease exponentially at large qR_g, while the amplitude of the mode with $p = 3$ approaches a constant value for large qR_g.

Figure 4 shows the calculated relaxation rates for the lowest six modes of an asymmetric diblock copolymer plotted as the open symbols in units of $\pi^2/(4t^*)$ vs qR_g. For comparison, also shown in Figure 4 are α_p^2/t^*, for $p = 1, 2, 3, ...$, as the dashed lines. In the small-qR_g limit, the relaxation rates are given by $\Gamma_{p,\beta} \simeq (2p - 1)^2\pi^2/(4t^*)$, $p = 1, 2, 3...$ and $\Gamma_{p,\alpha} \simeq (2p - 2)^2\pi^2/(4t^*)$, $p = 2, 3....$ As qR_g increases, the $\Gamma_{p,\beta}$ rates follow $\Gamma_{p,\beta} = \beta_p^2/t^*$. On the

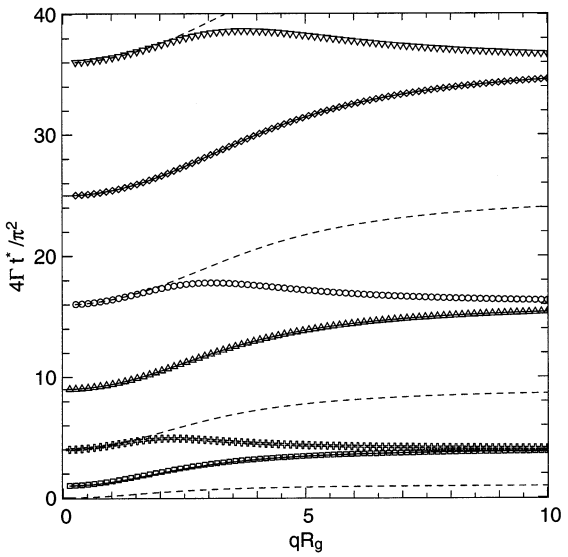

Figure 4. Calculated relaxation rates for the lowest six modes of a noninteracting, asymmetric diblock copolymer plotted in units of $\pi^2/(4t^*)$ vs qR_g. Dashed lines correspond to α_p^2/t^*.

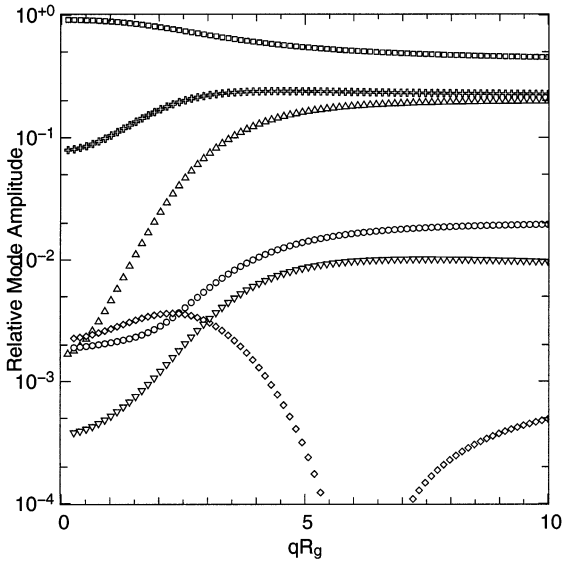

Figure 5. Calculated relative mode amplitudes for the lowest six modes of a moderately asymmetric ($f = 0.30$) diblock copolymer vs qR_g, corresponding to the relaxation rates shown in Figure 4.

other hand, the $\Gamma_{p,\alpha}$ rates only equal α_p^2/t^* at small qR_g. As qR_g increases, these relaxation rates soon deviate from the dashed curves, increasing only slightly with increasing qR_g to reach a maximum near $qR_g \simeq 2.5$. With further increase of qR_g, the $\Gamma_{p,\alpha}$ rates decrease to approach $\Gamma_{p,\alpha} \simeq (2p - 2)^2\pi^2/(4t^*)$, $p = 2, 3, ...$, at large qR_g.

The corresponding mode amplitudes for $f = 0.3$ are shown in Figure 5 plotted on a logarithmic scale vs qR_g plotted on a linear scale. In this case, the $\Gamma_{1,\beta}$-mode has the largest relative amplitude for all qR_g. It starts off at small qR_g with an amplitude near unity, but decreases to reach about 0.5 at large qR_g. At the same time, the $\Gamma_{2,\alpha}$-mode and the $\Gamma_{3,\alpha}$-mode increase to achieve values of about 0.2 at large qR_g.

Although the calculated relaxation rates of for an asymmetric diblock copolymer are independent of f, the mode amplitudes depend strongly on f. Shown in Figure 6 are the relative amplitudes of the lowest six modes

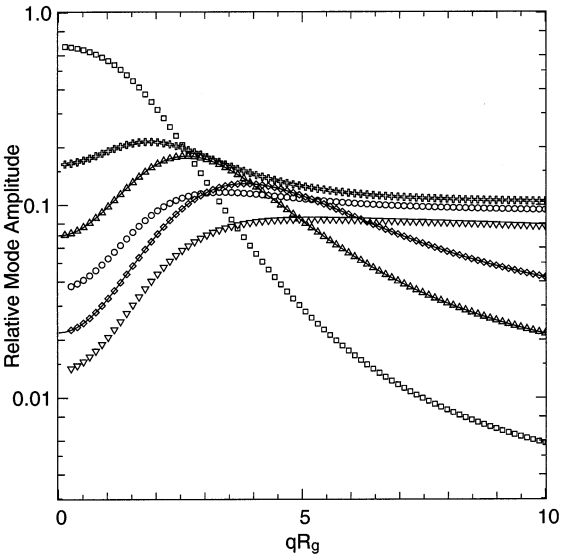

Figure 6. Calculated relative mode amplitudes for the lowest six modes of a highly asymmetric diblock copolymer with $f = 0.05$ vs qR_g, corresponding to the relaxation rates shown in Figure 4.

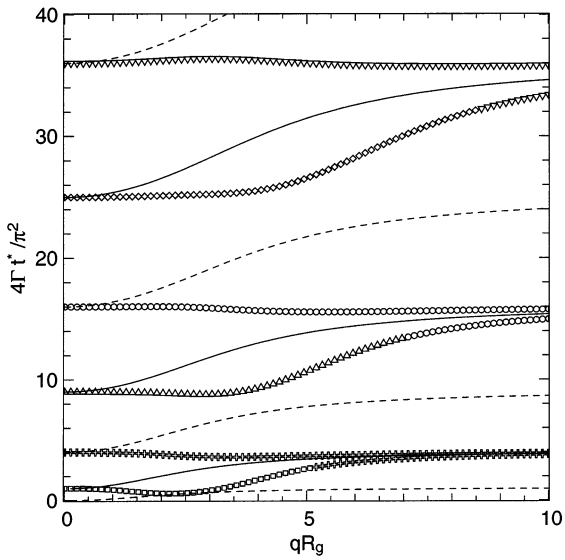

Figure 7. Calculated relaxation rates for the lowest six modes of an interacting asymmetric diblock copolymer with $f = 0.05$ and $\chi = 0.23$ plotted in units of $\pi^2/(4t^*)$ *vs* qR_g. Solid and dashed lines correspond to the single chain poles β_p^2/t^* and α_p^2/t^*, respectively.

for $f = 0.05$, which are very different from the relative amplitudes for $f = 0.30$. For $f = 0.05$, although the $\Gamma_{1,\beta}$-mode is dominant in the small-qR_g limit, its amplitude decreases rapidly with increasing qR_g, while the amplitudes of higher order modes increases. Thus, near the peak of the static structure factor ($qR_g \simeq 2.5$), it may be seen that there are three modes with roughly comparable intensity (namely the $\Gamma_{1,\beta}$, $\Gamma_{2,\beta}$, and $\Gamma_{2,\alpha}$-modes). It follows that the ISF for a noninteracting highly asymmetric diblock is highly non-single-exponential.

The effect of chemical interactions may be incorporated straightforwardly by introducing the usual Flory–Huggins interaction parameter (χ). Then, within the dRPA, the dynamic response function in the presence of interactions is given by

$$\frac{1}{\kappa(q,s)} = \frac{1}{\kappa_0(q,s)} - 2\chi \qquad (24)$$

To illustrate the effect of chemical interactions when these interactions are as large as possible, we have chosen to examine a value for the interaction parameter ($\chi = 0.23$) that lies near the stability limit of the homogeneous phase. Figure 7 shows the calculated relaxation rates of the lowest six modes of an asymmetric diblock copolymer with $f = 0.05$ and $\chi = 0.23$. Evidently, they are significantly changed from the noninteracting case. Interestingly, $\Gamma_{1,\beta}$ decreases as qR_g increases from zero to reach a minimum near the peak of the static structure factor (bottom panel of Figure 1) at $qR_g \simeq 2.5$. Presumably, this reflects the general phenomenon, known as de Gennes narrowing, that particularly free-energetically favorably configurations, as signaled by a peak in the static structure factor, also are particularly long-lived, as signaled by a minimum in their relaxation rate.[23]

Figure 8 shows the corresponding mode amplitudes. Clearly, the predominant position of the $\Gamma_{1,\beta}$-mode has been recovered, so that near the limit of the stability of the homogeneous phase, the IFS is nearly single-exponential once more.

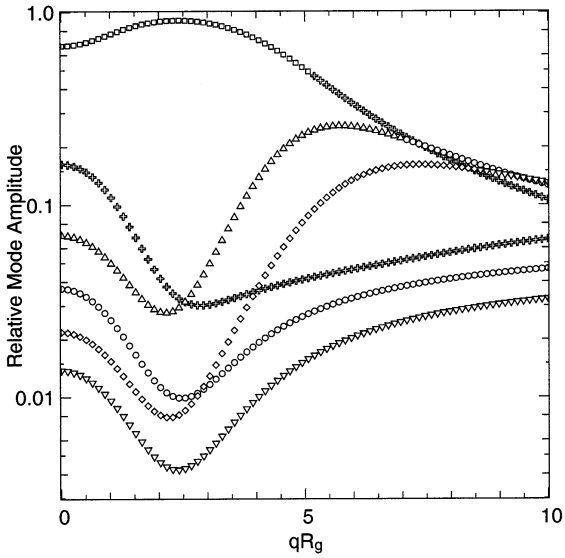

Figure 8. Calculated mode amplitudes for the lowest six modes of an asymmetric diblock copolymer with $f = 0.05$ and $\chi = 0.23$, corresponding to the relaxation rates shown in Figure 7.

Conclusions

We have given an explicit expression for the ISF of a melt of asymmetric diblock copolymers, calculated within the dynamic random phase approximation. Using this form, we have shown that the spectrum of relaxation rates for this system consists of two sets of modes. One set ($\Gamma_{p,\beta}$) is present in all cases. The other set of modes ($\Gamma_{p,\alpha}$) only appears in the case of asymmetric diblocks. In the noninteracting case, the relaxation rates of both sets of modes are independent of diblock composition (f) with $\Gamma_{p,\beta} = \beta_p^2/t^*$ at all qR_g, with β_p given by the pth positive root of $\beta_p \cot \beta_p - (qR_g)^2/2 = 0$, and $\Gamma_{p,\alpha} = (\pi^2/4t^*)(2p - 2)^2$ for $p = 2, 3, 4, ...$, in both the small-qR_g and large-qR_g limits. In contrast, the mode amplitudes depend strongly on f. In addition, the ISF becomes increasingly non-single-exponential at the peak of the static structure factor for increasingly asymmetric

compositions. These results may be valuable in interpreting the results of future scattering experiments, especially PCS studies of solutions of asymmetric very-long-chain diblocks, and XPCS studies of melts of asymmetric diblocks. Indeed, as advertized above, these results suggest that careful scattering studies, performed on asymmetric block copolymers, may afford an excellent opportunity to evaluate quantitatively the reptation model's detailed predictions for the higher-order mode relaxation rates and relative mode amplitudes. This is not only because of the predicted non-single-exponential relaxation of the ISF for very asymmetric block copolymers, but also because of the ppoint that when investigating entanglement effects, which become increasingly inportant as N increases, it is experimentally convenient that a diblock with a given Flory−Huggins interaction parameter (χ) remains in the homogeneous phase up to larger values of N for f far from $^1/_2$ than for f near $^1/_2$. For example, the instability toward phase separation occurs at $\chi N \simeq 10$ for $f \simeq 1/2$ but at $\chi N \simeq 250$ for $f \simeq 0.05$.

Acknowledgment. This work was supported by the NSF via Grant DMR 0071755, and was motivated by experimental work carried out in collaboration with Adrian Ruehm, Hyunjung Kim, Larry Lurio, Sunny Sinha, Jyotsana Lal, and Joydeep Basu. I thank D. Lumma and a reviewer for valuable comments and suggestions.

References and Notes

(1) Bates, F. S.; Fredrickson, G. H. *Annu. Rev. Phys. Chem.* **1990**, *11*, 525−557.
(2) Bates, F. S.; Fredrickson, G. H. *Phys. Today* **1999**, *52* (2), 32−38.
(3) Thompson, R. B.; Ginsberg, V. V.; Matsen, M. W.; Balazs, A. C. *Macromolecules* **2002**, *35*, 1060−1071.
(4) Fasolka, M.; Harris, D. J.; Mayes, A. M.; Yoon, M.; Mochrie, S. G. J. *Phys. Rev. Lett.* **1997**, *79*, 3018−3021.
(5) Anastasiadis, S. H. *Curr. Opin. Colloid Interface Sci.* **2000**, *5*, 324−333.
(6) Semenov, A. N.; Anastasiadis, S. H.; Boudenne, N.; Fytas, G.; Xenidou, M.; Hadjichristidus, N. *Macromolecules* **1997**, *30*, 6280−6294.
(7) Erukhimovich, I. Y.; Semenov, A. N. *Sov. Phys. JETP* **1986**, *63*, 149−156.
(8) de Gennes, P. G. *J. Chem. Phys.* **1971**, *55*, 572.
(9) Doi, M.; Edwards, S. F. *J. Chem. Soc., Faraday Trans.* **1978**, *74*, 1789.
(10) Doi, M.; Edwards, S. F. *The Theory of Polymer Dynamics*; Oxford University Press: Oxford, England, 1986.
(11) Lumma, D.; Borthwick, M. A.; Falus, P.; Lurio, L. B.; Mochrie, S. G. J. *Phys. Rev. Lett.* **2001**, *86*, 2042−2045.
(12) Lumma, D.; Mochrie, S. G. J. *Macromolecules* **2001**, *34*, 8303−8314.
(13) de Gennes, P. G. *J. Phys. (Paris)* **1981**, *42*, 735.
(14) Richter, D.; Farago, B.; Fetters, L. J.; Huang, J. S.; Ewen, B.; Lartigue, C. *Phys. Rev. Lett.* **1990**, *64*, 1389−1392.
(15) Richter, D.; Butera, R.; Fetters, L. J.; Huang, J. S.; Farago, B.; Ewen, B. *Macromolecules* **1992**, *25*, 6156−6164.
(16) Schleger, P.; Farago, B.; Lartigue, C.; Kollmar, A.; Richter, D. *Phys. Rev. Lett.* **1998**, *81*, 124−127.
(17) Wischnewski, A.; Monkenbusch, M.; Willner, L.; Richter, D.; Likhtman, A. E.; McLeish, T. C. B.; Farago, B. *Phys. Rev. Lett.* **2002**, *88*, 058301-1−058301-4.
(18) Akcasu, A. Z.; Benmouna, M.; Benoit, H. *Polymer* 1986, *27*, 1935.
(19) Forster, D. *Hydrodynamic Fluctuations, Broken Symmetry, and Correlation Functions*; Benjamin: Reading, MA, 1975.
(20) Higgins, J. S.; Benoit, H. C. *Polymers and Neutron Scattering*; Oxford University Press: Oxford, England, 1994.
(21) Leibler, L. *Macromolecules* **1980**, *13*, 1602.
(22) Gradshteyn, I. S.; Ryzhik, I. M. *Table of Integrals, Series, and Products*; Academic Press: New York, 1965.
(23) de Gennes, P. G. *Physica* **1956**, *25*, 825−839.

MA020565A